



Effect of Ni Interlayer on the Interface Toughening and Thermal Stability of Cu/Al/Cu Clad Composites

Hyung Jin Kim¹ · Sun Ig Hong¹

Received: 26 February 2018 / Accepted: 17 July 2018 / Published online: 25 July 2018
© The Korean Institute of Metals and Materials 2018

Abstract

The effect of Ni interlayer on the interface toughening and stability of Cu/Al/Cu clad composite was studied. The peel strength of Cu/Al/Cu composite with Ni interlayer increased with increase of Ni thickness and reached 10.9 N/mm for the composite with 25 μm thick interlayer. The presence of periodic Ni interlayer between Cu and Al hinders the steady crack growth along Cu/Al interface and toughen the interface by inducing the crack deflection away from Cu/Al interface. The peel stress-displacement curves of as-roll-bonded clad exhibited the stress undulation and its amplitude increased with increase of nickel interlayer thickness. The degree of crack deflection was observed to increase with increasing nickel interlayer thickness. The peel strength of Cu/Al/Cu with 25 μm thick Ni interlayer increased up to 14.5 N/mm after annealing at 200 °C, greater than those observed in Cu/Al/Cu with no interlayers. The enhanced Cu/Al bonding and softening of Al matrix by annealing at 200 °C further increased the peel strength because the crack propagated continuously through the ductile Al plate. The formation of pronounced intermetallic compounds at Cu/Al and Ni/Al interfaces after annealing above 400 °C induced the crack growth along the layers of brittle intermetallics and reduced the beneficial effects of Ni interlayer.

Keywords Crack deflection · Ni interlayer · Cu/Al/Cu · Interface · Composite · Peel strength

1 Introduction

The interest in layered copper–aluminum clad composites has been surging in the electronics and automobile industry because of their recent power electronic and wiring applications [1–5]. The advantages of replacing copper and copper alloys with Cu/Al clad composite are the high specific strength, good electrical and thermal conductivities, reduced weight and price competitiveness over copper and copper alloys [4–7]. Cu/Al clad composites with good conductivity and low density are now being considered for use as conductors or heat exchangers in vehicular, electronic and energy-sector applications [6]. Cu/Al hybrid leadframes are currently used in steering control, anti-lock braking and air bag control systems [8]. Roll-bonding has been widely used because it is a reliable, cost-efficient and mass production process [4–9].

Technological challenge in metal cladding and joining is to obtain the interface with reliable bonding strength [10, 11] and to control the interfacial intermetallic formation. Post-roll-bonding annealing is often required for subsequent forming parts and products with various shapes. Aluminum and copper form brittle intermetallics [12–19] at high temperatures, which are known to induce easy delamination and interface fracture and even deteriorate the electrical conductivity [5, 14]. The post-roll-bonding annealing process conditions which optimize the interface strength of roll-bonded clad without excessive formation of interfacial intermetallics needs to be established [20–27]. In order to find a way to enhance the interface strength and interface stability, the effect of metal interlayers such as Ni and Cu have been studied for Cu/Al [28] and Al/Mg [29] clad composites. Ni interlayer in Cu/Al clad may act as diffusion and reaction barriers because nickel has a lower diffusivity in Al and does not form intermetallic compounds with Cu.

For application Cu/Al clads in electronic and electrical components, materials engineers are warned to avoid applications where components are exposed to excessive heat (above 250 °C) for a prolonged period time or to very high temperatures [9]. For the application of Cu/Al clad in

✉ Sun Ig Hong
sihong@cnu.ac.kr

¹ Department of Nanomaterials Engineering, Chungnam National University, Daejeon 34134, Republic of Korea

a harsher thermal environment, Cu/Al clads with improved interface strength and thermal stability need to be developed. Recently, Shabani et al. [28] studied the influence of electroplated Ni layer on Cu on the interface structure and bond strength of Cu/Al clad. The understanding on the effect of Ni interlayer on the interface strength regardless of its positive or negative nature is not well understood. In this study, the effect of Ni interlayer on the interface strength and the nature of interaction between layers of Cu, Ni and Al in roll-bonded Cu/Al/Cu with Ni interlayers were examined and characterized. The optimization of interface strength by post-roll-bonding heat treatments was also carried out to find a way to improve the interface strength through interface modification.

2 Experimental Procedure

In this study, layered Cu/Al/Cu clad and those with Ni interlayers between Cu and Al was fabricated using roll bonding process. Metals used for roll-bonding were deoxidized copper [0.002% O, 0.015% P, 0.002% Zn, balance Cu (99.9% purity)] and 1060 aluminum of the commercial purity [0.20% Si, 0.05% Cu, 0.25% Fe, balance Al (99.4% purity)]. In order to investigate the effect of Ni interlayers, annealed Cu plates were electroplated with nickel. Electroplating was carried out using an applied voltage of 8 V in the electrolyte solution consisting of nickel chloride (NiCl₂), nickel sulfate (Ni₂SO₄) and boric acid (H₃BO₄). Electroplating time was adjusted to obtain the targeted thicknesses (5, 13, 25 μm) of Ni interlayer after roll-bonding. In order to analyze the thickness, continuity, and uniformity of Ni coating layer prior to rolling, the edge view of the Ni-electroplated Cu plate with the targeted thickness of 5 μm (a), 13 μm (b) and 25 μm (c) was examined (Fig. 1). As shown in Fig. 1, defect- and crack-free Ni layer was formed on the Cu plates. The exact thickness of the nickel coating layers before cladding was determined to be 5.64 ± 0.31 μm, 16.72 ± 0.35 μm and 37.30 ± 0.97 μm cross-sectional micrographs of scanning electron microscopy. Stacked Al plate between two nickel

electro-plated Cu were roll-bonded at a reduction ratio of 60.5% in one pass at room temperature. The final thickness of clad composite plate was 2.0 mm and those of Al and Cu sheets were approximately 1.6 and 0.2 mm, respectively.

The final thickness of the nickel interlayer after cold-roll-bonding were reduced to 5.20 ± 0.24 μm, 13.08 ± 1.25 μm and 24.04 ± 1.27 μm, close to the targeted thicknesses. The thicknesses of electroplated Ni coating and post-roll-bonding Ni interlayer are summarized in Table 1. The bond strength between Al and Cu was measured by peel test in accordance with ASTM D1876. The crosshead speed for the peel test was carried out at the speed of 1 mm/min and interface structures of layered Cu/Al/Cu clad composites without and with Ni interlayers were characterized by a scanning electron microscope (SEM). To identify the phases in thin intermetallic layers at the interface more precisely, X-ray diffraction (XRD) analyses and energy dispersive X-ray spectroscopy (EDS) were performed on the fractured surfaces of separated Cu and Al interfaces after peel test.

3 Results and Discussion

3.1 Effect of Ni Interlayer Thickness on the Peel Strength

Figure 2 displays the peel strength-displacement curves of roll-bonded Cu/Al/Cu composite plate without and with Ni interlayers. In Fig. 2, the peel stress was defined as the average peel force divided by the width of the specimen

Table 1 Thicknesses of electroplated Ni coating and post-roll-bonding Ni interlayer

Targeted thickness (μm)	Coated thickness (μm)	Post-roll-bonding thickness (μm)
5 um Ni	5.64 ± 0.31	5.2 ± 0.24
13 um Ni	16.72 ± 0.35	13.08 ± 1.25
25 um Ni	37.3 ± 0.97	24.04 ± 1.27

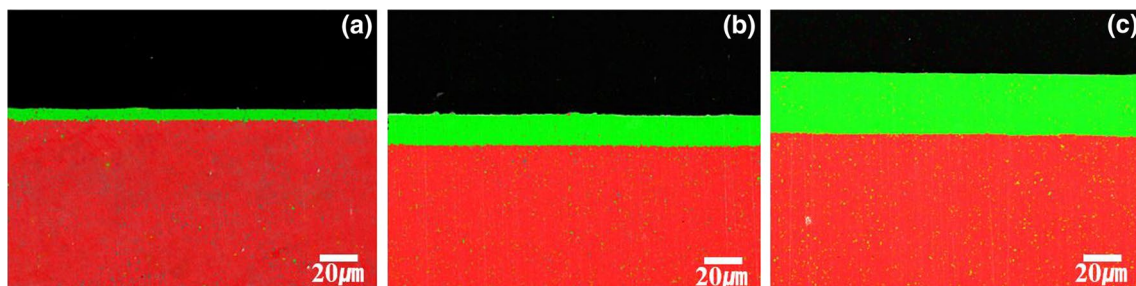


Fig. 1 Edge view (EDS image) of the Ni-electroplated Cu plate with the targeted thickness of 5 μm (a), 13 μm (b) and 25 μm (c). Continuous and uniform crack-free Ni coating layer was formed

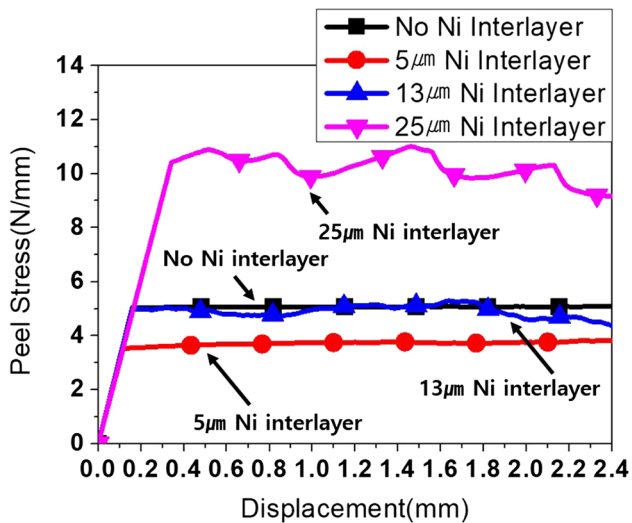


Fig. 2 Peel strength-displacement curves of as-roll-bonded Cu/Al/Cu composite plate without and with Ni interlayers

(gage width) [6, 8, 28]. Cu/Al/Cu clad composite without Ni interlayer and Cu/Al/Cu clad with 5 μm thick interlayer exhibit quite stable strength-displacement curve. It is interesting to note that the peel strength decreased with the presence of 5 μm thick Ni interlayer. Another interesting observation is that gentle undulation with relatively long wave length were noticeable in Cu/Al/Cu with 13 μm thick interlayer and the amplitude of undulation (or serration) dramatically increased with increase of Ni interlayer thickness to 25 μm . The peel stress of roll-bonded Cu/Al/Cu with 25 μm thick interlayer decreased from 10.9 N/mm to

9.1 N/mm with increase of displacement. The peel strength of as-roll-bonded Cu/Al plate with a cold reduction of 57% observed by Chen et al. [7] reached 6.3 N/mm initially and then stabilized at 2.2 N/mm. Peng et al. [30] reported the peel stress of Cu/Al clad increased up to 5.9 N/mm after warm rolling reduction of 60% (430 $^{\circ}\text{C}$). Compared to the results of other investigators [7, 30] and the peel strength of Cu/Al/Cu without Ni interlayer in the present study, the peel strength of as-roll-bonded Cu/Al/Cu with thick Ni interlayer (> 15 μm) was found to be greater. The peel strength of Cu/Al/Cu plate with Ni interlayers improved further by post-roll-bonding heat treatment and will be discussed below.

Figure 3a–f exhibit SEM images (a–c) and EDS elemental mapping images (d–f) of separated Cu/Al interface region with Ni interlayers of 5 μm (a, d), 13 μm (b, e) and 25 μm (c, f) in the partially peeled off clad plate. In the EDS elemental mapping images (Fig. 3d–f), Cu, Al and Ni is displayed in red, blue and green color respectively. As shown in Fig. 3, the interface between Cu and Al is not fully covered by Ni layer, suggesting electroplated Ni on the Cu sheet is less ductile [31] and fractured between Cu and Al plates during clad roll-bonding. It should also be noted that fragmented Ni interlayer remains on the Cu plate after peel test because Cu/Ni bonding by electroplating is stronger than mechanical Ni/Al bonding during clad-roll-bonding. The examination of the interface region of Cu plate revealed that the size of fragmented Ni interlayer and the distance between fragmented Ni interlayer (i.e. the width of Ni-layer free Cu region) increased with increase of Ni interlayer thickness. The increasing size of

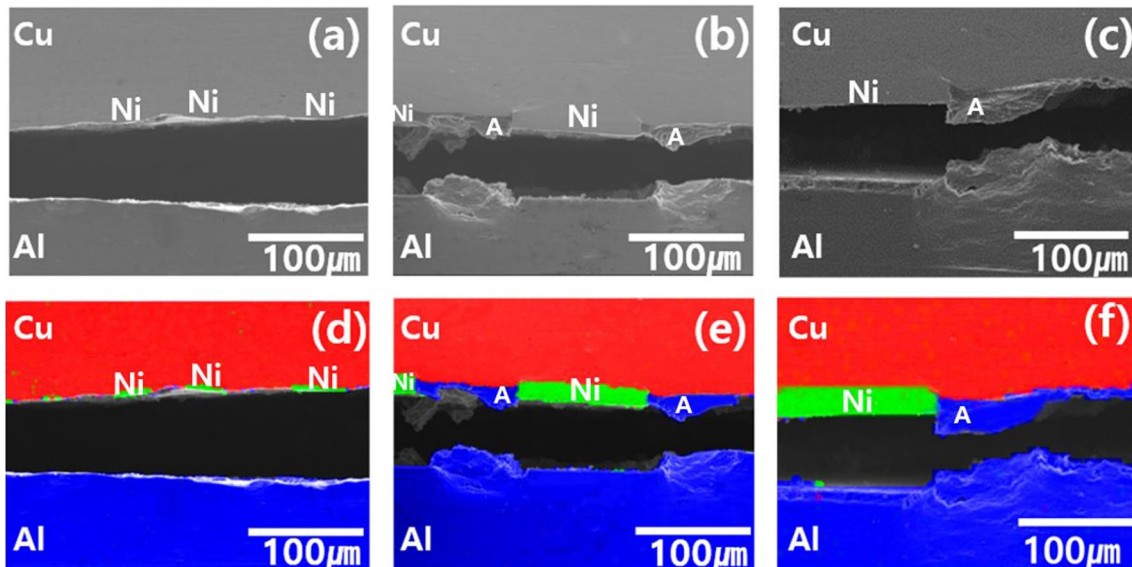


Fig. 3 SEM images (a–c) and EDS elemental mapping images (d–f) of separated Cu/Al interface region with Ni interlayers of 5 μm (a, d), 13 μm (b, e) and 25 μm (c, f) in the partially peeled off clad plate. (Color figure online)

fragmented Ni interlayer is due to the increase of the load required to fragment thicker Ni layer into pieces.

One interesting observation in Fig. 3 is the presence of heavily distorted Al lumps (marked with “A”) torn-off from Al plate and attached to the separated Cu plate and the volume of torn-off Al lump detached from Al plate increased in size with increase of Ni interlayer thickness. The smooth crack propagation along the same interface level is not possible in the presence of Ni interlayer because the height level of Ni/Al interface (along which crack propagates) is higher than the level of Cu/Al interface by the thickness of Ni interlayer. The presence of heavy deformation markings and slip lines in the torn-off Al lumps detached from Al plate in Fig. 3b, c should be noted. In Fig. 3, the interface crack propagating close to the Cu/Al interface in the region with no Ni interlayer would deflect and deviate away from the Cu/Al interface as the crack approached the region with Ni interlayer because of strong Cu/Ni interface bonding. The deflection of propagating crack away from Cu/Al interface would induce heavy deformation of Al plate in front of crack tip and increase the peel strength. Since the degree of crack deflection increases with increasing Ni interlayer thickness, the amplitude of undulation (or serration) increased with increasing Ni interlayer thickness and more energy is needed to propagate the crack, resulting in the high peel strength.

Figure 4a–c display the EDS elemental map images of fracture surface of peeled off Cu plate with Ni interlayers of 5 μm (a), 13 μm (b) and 25 μm (c). In this figure, Cu, Al and Ni is displayed in red, blue and green color respectively. The size of fragmented pieces of Ni interlayer (green) increased with increase of Ni coating thickness as shown in Figs. 3 and 4 because thicker Ni layer could withstand the higher load during roll-bonding. The peeled-off fracture surface of Cu plate revealed three colored regions; irregular shaped Ni interlayer polygons with no distinctive surface feature and the inter-connected irregular shaped areas mixed with Cu and Al regions. The increase of Al regions (blue) on the peeled-off fracture surface of Cu plate with increase of Ni interlayer thickness in Fig. 4 suggests that more heavily deformed Al lumps were detached from Al plate and attached to Cu plate.

The ridge-like pattern in Al developed more pronouncedly and clearly with increase of Ni interlayer thickness. The ridge-like pattern with dimples developed during fracture by necking and shearing of the Al matrix metallic-bonded to Cu plate because crack propagated through Al not along Cu/Al interface. It should also be noted that the Cu regions (red) in Fig. 4c is much less than Al regions (blue) even though Fig. 4c shows the fracture surface image of the peeled-off Cu plate. The surface of Ni interlayer detached from Al plate in Fig. 4 was observed to be rougher with increased linear markings and Al debris (blue) with increasing Ni thickness, implying Ni/Al bonding was enhanced with Ni thickness. The most pronounced ridge-like pattern with dimples on the peeled-off surface of Cu plate with Ni interlayers of 25 μm suggest that a significant energy was absorbed for separation of Cu and Al plates during the peel test.

In order to find the reason for the increased amplitude of undulation (or serration) in the peel stress versus displacement curves, successive stereomicroscopic image and SEM image of Al side of Cu/Al/Cu clad composites with Ni interlayers (13 and 25 μm) undergoing the peel tests were observed. In Fig. 5a, the edge view of the peeled-off Al plate observed by SEM, showing the interface fracture features of Cu/Al/Cu clad with 25 μm Ni interlayer are displayed. Some important features are marked with “A–G”, which matches one by one to the undulations in the peel stress versus displacement curve in Fig. 5b. In Fig. 5a, relatively flat fracture surface regions (regions “CD” and “EF”) are those that were in contact with Ni interlayer and protruded regions are those with torn-off Al lumps. In Fig. 5a, peel stress stayed low as the crack front passed through the region with Ni interlayer and entered the Ni-layer-free region and propagated close to Cu/Al interface (for example, the point marked with D or F). The peel stress started to increase as it deviated away and deflected into Al matrix and propagated through the Al matrix away from Cu/Al interface. The peel stress reached the peak as the crack deflected further from Cu/Al interface as it approached the points (for example, marked with E or G) where fragmented Ni interlayers are present.

It is apparent that crack propagating along Cu/Al interface deflected and deviated from Cu/Al interface because of

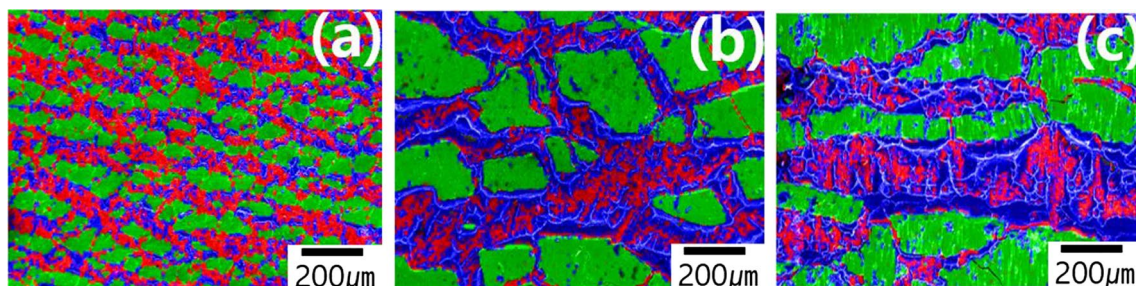
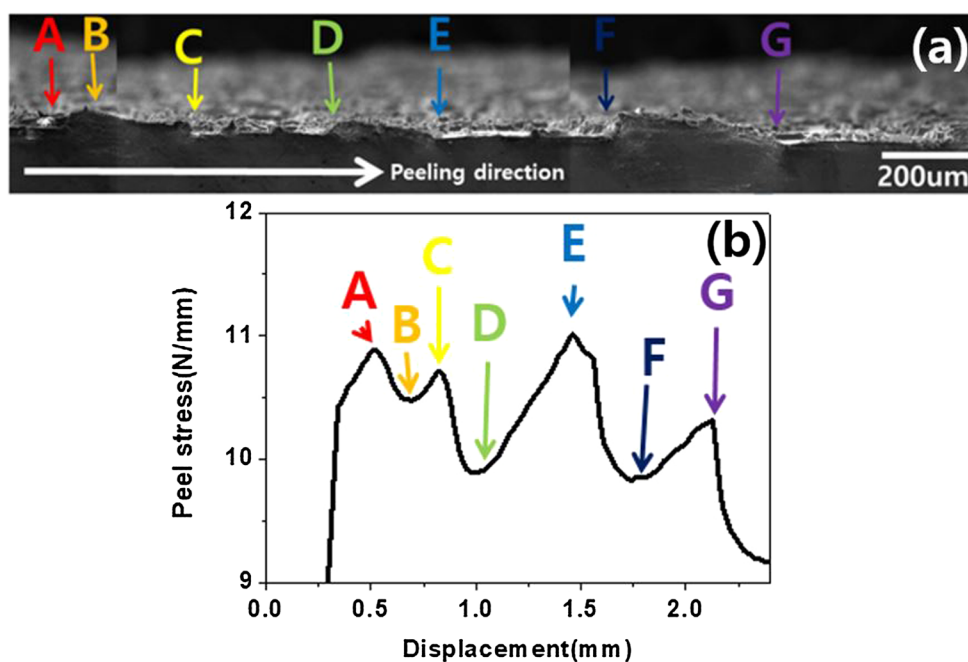


Fig. 4 EDS elemental map images of fracture surface of peeled off Cu plate with Ni interlayers of 5 μm (a), 13 μm (b) and 25 μm (c). (Color figure online)

Fig. 5 **a** Interface fracture features in the edge view of the fracture surface of peeled-off Al plate in Cu/Al/Cu clad with 30 μm Ni interlayer observed by SEM, **b** peel stress versus displacement curve with undulations matched one by one to the features marked on the fracture surface



strong Cu/Ni interface bonding as the crack front approaches the points C, E, and G. The periodic crack deflection would increase the crack propagation energy, resulting in the enhanced peel strength. Shabani et al. [28] observed a significant decrease of the bonding strength in the presence of thin Ni interlayer in the layered Cu/Al clad plates and the enhanced interface bonding strength in the clad plates with thicker Ni interlayer. They attributed the increased bonding strength for Cu/Al clad plates with thicker Ni interlayer to a large volume of metal extruded through the wider cracks of Ni layer, creating strong bonds with the opposite layer [28]. The correlation between the amplitude of undulation and the degree of crack deflection in the present study, however, strongly suggests that the enhanced toughening with increasing Ni interlayer thickness is associated with crack deflection away from Cu/Al interface, requiring more energy for crack propagation.

Figure 6 shows the X-ray diffraction peaks from the peeled-off fracture surface of Cu plate. Diffraction spectra from the peeled-off fracture surface of Cu plate exhibited peaks from Al and Ni as well as that of Cu. One of the most interesting observations in this figure is the increase of Al peaks with the increase of Ni interlayer thickness, suggesting that the volume of Al torn off from Al plate and attached to Cu plate during crack propagation increased. Another interesting observation is that (111) and (200) Al peaks increased more drastically in intensity with increase of Ni interlayer thickness in comparison with that of (220) Al peak, implying that Al volume attached on to Cu plate has the heavily deformed $\langle 111 \rangle$ and $\langle 200 \rangle$ texture. The

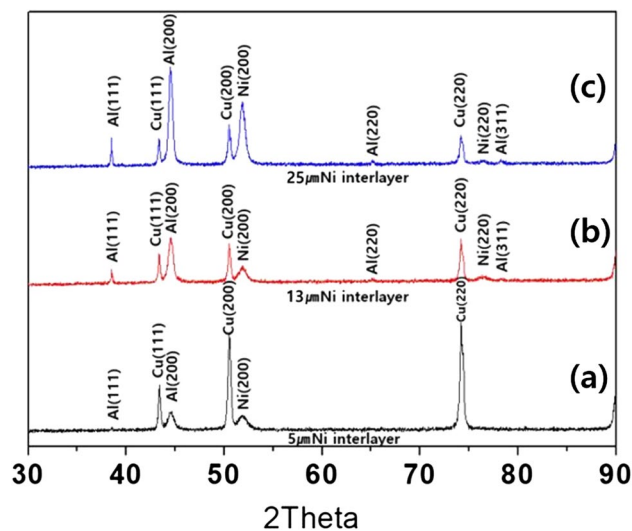


Fig. 6 X-ray diffraction peaks from the peeled-off fracture surface of Cu plate in Cu/Al/Cu clad composites with Ni interlayers of 5 μm (a), 13 μm (b) and 25 μm (c). Diffraction spectra from the peeled-off fracture surface of Cu plate exhibited peaks from Al and Ni as well as that of Cu

[100] component was attributed to the first-order deformation twinning of the [111] component [32–36]. The enhanced development of (111) and (200) Al peaks with increasing thickness of Ni interlayer on the fractured surface of Al plate was also observed in the present study (XRD not shown).

3.2 Effect of Annealing on the Interface Structure

Figure 7a–f exhibit the SEM images and elemental mapping images of interface region of Cu/Al/Cu clad (with 25 μm Ni interlayer) annealed at 200 $^{\circ}\text{C}$ (a, e) 300 $^{\circ}\text{C}$ (b, f), 400 $^{\circ}\text{C}$ (c, g) and 500 $^{\circ}\text{C}$ (d, h). SEM image of as-roll-bonded layered Cu/Al/Cu clad is very similar to that annealed at 200 $^{\circ}\text{C}$ and will not be shown. In these figures, Cu, Al and Ni are displayed in red, blue and green respectively. The intermetallic compounds in the clad composite is marked as “IMC” in Fig. 7a–d. After annealing at 200 $^{\circ}\text{C}$ as shown in Fig. 7a, e, no intermetallic compounds at Cu/Al and Ni/Al interfaces were visible. After annealing at 300 $^{\circ}\text{C}$ (b, f), thin intermetallic compound layer was obviously formed in the Cu/Al interface region without Ni layer, but no intermetallics were visible at the Ni/Al interface. In Fig. 7c, d, g, h, the intermetallic compounds were observed both at Cu/Al and Ni/Al interfaces after heat treatments at 400 and 500 $^{\circ}\text{C}$, but thickness of the intermetallic layer was much thicker at the Cu/Al interface. The intermetallic phases at the Cu/Al interface were identified to be Cu_9Al_4 , CuAl and CuAl₂ previously by many investigators [5–9, 13, 14, 21, 37]. One consequence of fast growing intermetallic at the Cu/Al interface is that the height level of Ni/Al interface in the region with Ni interlayer is close to the level of intermetallic/Al interface in the region without Ni interlayer as shown in Fig. 7d, h.

The thickness of intermetallic layers at the Cu/Al and Ni/Al interfaces are plotted against the heat treatment temperature in Fig. 8. The intermetallic layer thickness grew much slower with increase of temperature at the Ni/Al interface, suggesting the formation of intermetallic compounds was apparently suppressed in the region with Ni layer because of lower diffusivity of Ni in Al. Ni interlayer obviously acted as diffusion and reaction barrier between Cu and Al. In order

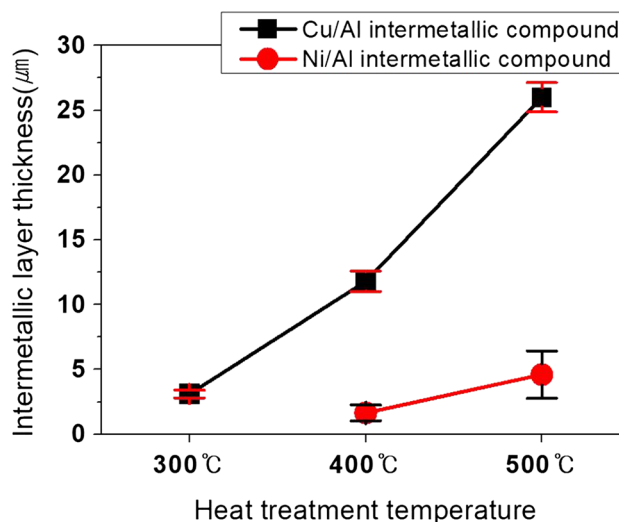


Fig. 8 Thickness of intermetallic layers at the Cu/Al and Ni/Al interfaces plotted against the annealing temperature

to identify the phases of thin intermetallic compounds with more accuracy, Cu/Al/Cu clad composite with Ni interlayers heat treated at 200, 300, 400 and 500 $^{\circ}\text{C}$ were separated by peel test. The separated fractured surfaces of Cu plate (a) and Al plate (b) were characterized by XRD. Figure 9a and 9b exhibit XRD peaks from the separated Cu and Al plates, respectively. As expected, no peaks from any intermetallic compound were observed after annealing at 200 $^{\circ}\text{C}$. The examination of XRD peaks demonstrate the presence of Cu_9Al_4 , CuAl, CuAl₂ and Ni_2Al_3 as well as Cu and Ni on the Cu side and CuAl₂, CuAl, Cu_9Al_4 and NiAl_3 as well as Al on the Al side after annealing at 500 $^{\circ}\text{C}$. At 400 $^{\circ}\text{C}$, Cu_9Al_4 and CuAl intermetallics as well as Cu, Al and Ni were observed on the Cu side and CuAl₂, CuAl and NiAl_3 as

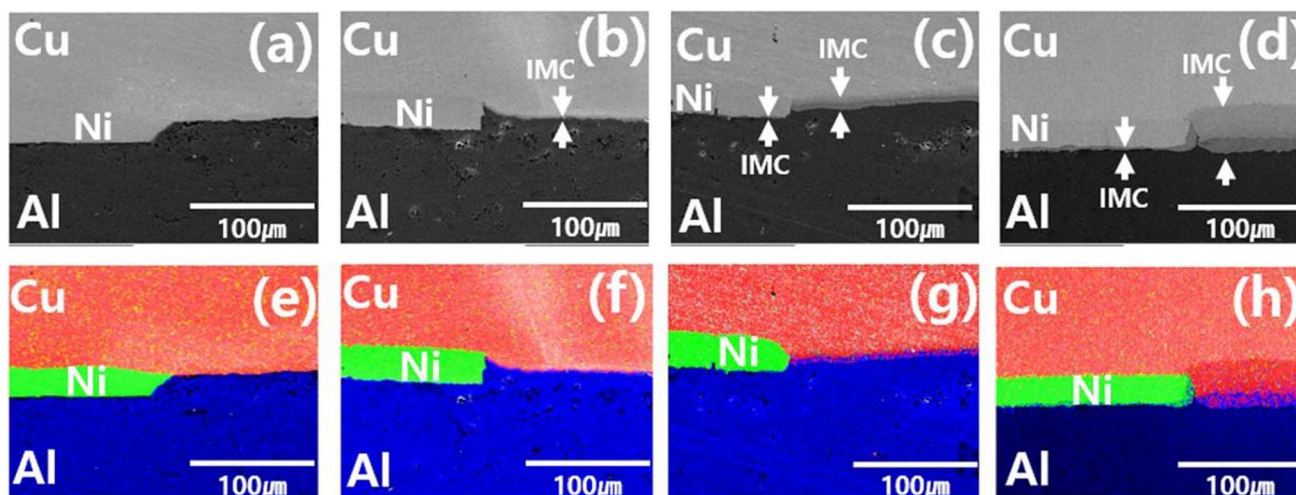


Fig. 7 SEM images and elemental mapping images of interface region of Cu/Al/Cu clad with 25 μm Ni interlayer. annealed at 200 $^{\circ}\text{C}$ (a, e) 300 $^{\circ}\text{C}$ (b, f), 400 $^{\circ}\text{C}$ (c, g) and 500 $^{\circ}\text{C}$ (d, h). (Color figure online)

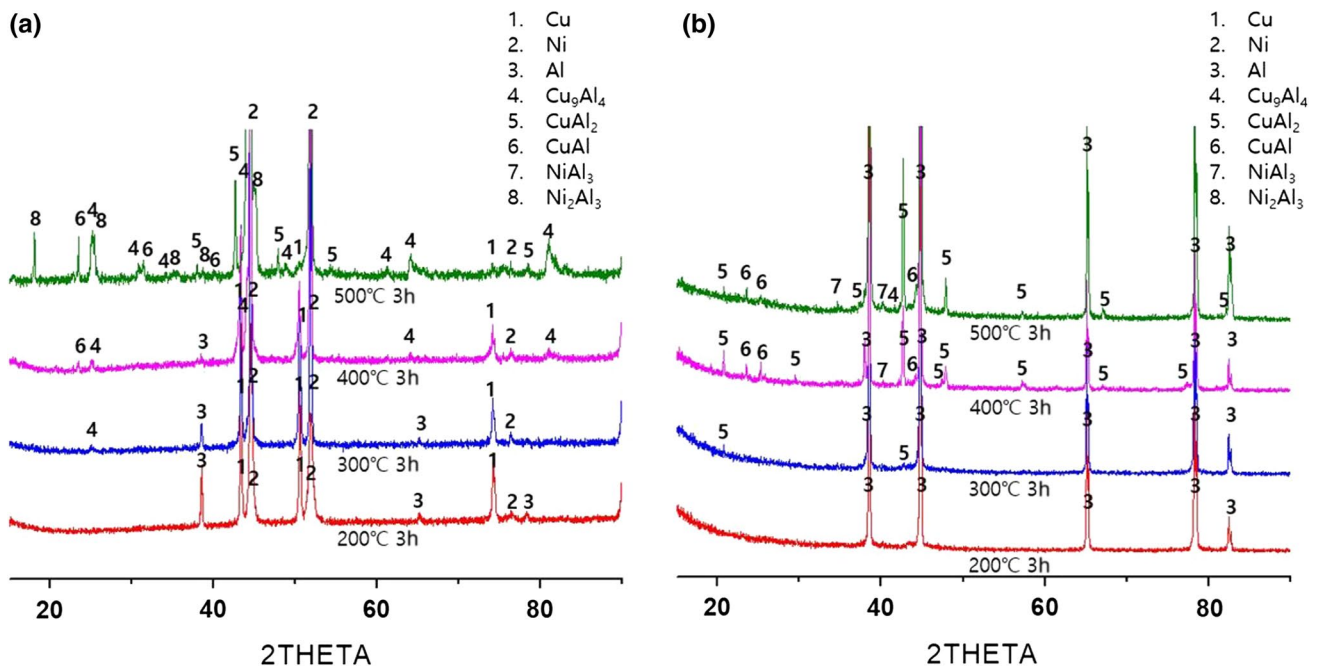


Fig. 9 XRD peaks from the separated Cu (a) and Al (b) plates annealed at 200, 300, 400 and 500 °C

well as Al were observed. Note that nickel aluminide intermetallic was only observed on the Al side after annealing at 400 °C. At 300 °C, Cu_9Al_4 intermetallics as well as Cu, Al and Ni were observed on the Cu side and CuAl_2 as well as Al were observed. XRD analyses supports the observation by SEM (Fig. 7) that intermetallic compounds formed at the Cu/Al interface, but no intermetallics formed at the Ni/Al interface after heat treatment at 300 °C.

3.3 Effect of Annealing on the Peel Strength

The peel strength-displacement curves of as-roll-bonded and annealed Cu/Al/Cu clad composites with 13 μm (a) and 25 μm Ni (b) interlayers are exhibited at Fig. 10a, b. The peel strength-displacement curves of Cu/Al/Cu with 5 μm Ni interlayer are not shown because the change of strength with annealing is not as pronounced as those with 13 and

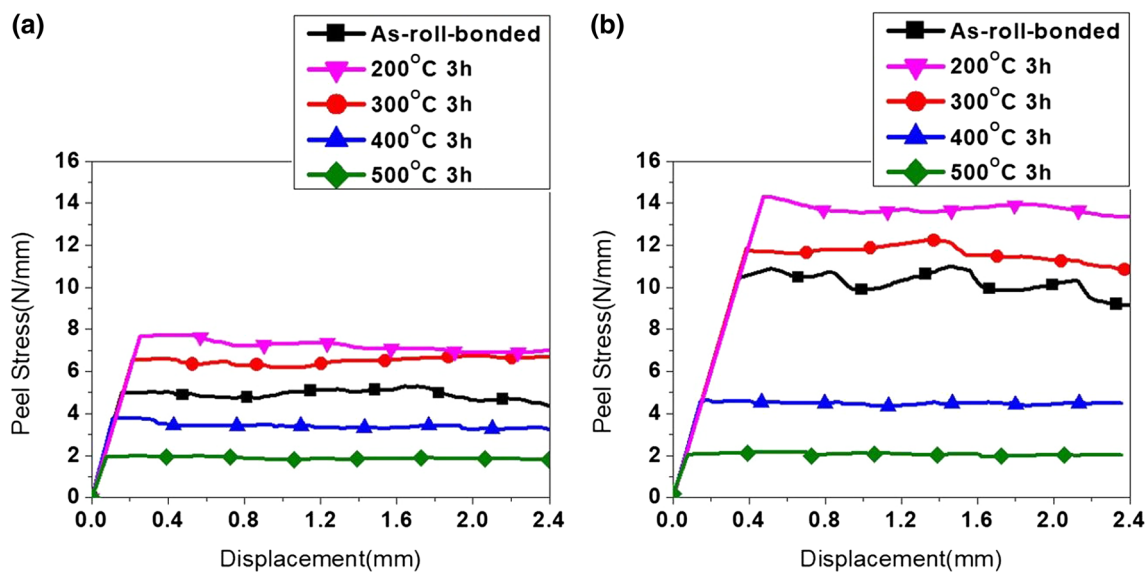


Fig. 10 Peel stress-displacement curves of as-roll-bonded and annealed Cu/Al/Cu composite plate with 13 μm (a) and 25 μm Ni (b) interlayer

25 μm Ni interlayers. The peel strength increased significantly (from 5.2 to 7.8 N/mm for Cu/Al/Cu with 13 μm Ni interlayer, 10.6–14.5 N/mm for Cu/Al/Cu with 25 μm Ni interlayer) after annealing at 200 $^{\circ}\text{C}$. The peel strength after annealing at 300 $^{\circ}\text{C}$ is slightly lower than that annealed at 200 $^{\circ}\text{C}$, but greater than that of the as-roll-bonded Cu/Al/Cu clad composite as shown in Fig. 10a, b. After annealing at 400 $^{\circ}\text{C}$, the peel strength decreased below that of the as-roll-bonded Cu/Al/Cu composite plate. One interesting observation in Fig. 10 is that the undulations (or serrations) in the peel stress-displacement curves of annealed Cu/Al/Cu composite plate became weaker after annealing at 200 and 300 $^{\circ}\text{C}$. It is interesting to note that the peel stress of Cu/Al/Cu composite plate with 25 μm Ni interlayer (Fig. 10b) decreased dramatically after annealing at 400 and 500 $^{\circ}\text{C}$ and became close to the stress levels observed in Cu/Al/Cu with 13 μm Ni interlayer (Fig. 10a). The similarity of the peel stress levels between Cu/Al/Cu clads with 25 and 13 μm Ni interlayers after annealing above 400 $^{\circ}\text{C}$ could be the formation of intermetallic layers at high temperatures. The peel stress-displacement curves after annealing at 400 and 500 $^{\circ}\text{C}$ exhibited the almost flat behavior because of the rather smooth crack propagation along intermetallic layers.

Figure 11a–d exhibit SEM images (a, b) and EDS elemental mapping images (c, d) of separated Cu/Al interface region with 25 μm Ni interlayer annealed at 200 $^{\circ}\text{C}$ (a, c) and 500 $^{\circ}\text{C}$ (b, d) in the partially peeled off clad plate. In the EDS elemental mapping images (c, d), Cu, Al and Ni is displayed in red, blue and green color respectively. The

presence of heavily distorted and torn-off Al lumps (marked with “A”) attached to the separated Cu plate and the volume of torn-off Al lump detached from Al plate suggests the strong bonding between Al and Cu. The diffusion across the Cu/Al interface with negligible intermetallic formation during annealing at 200 $^{\circ}\text{C}$ in Fig. 11a, c would increase the Cu/Al interfacial bonding. The enhanced Cu/Al interface bonding would prevent the crack propagation along the Cu/Al interface and induce cracking through Al matrix as shown in Fig. 11a, c, resulting in the significant increase of peel strength (Fig. 10b) associated with high crack propagation energy. The enhanced Cu/Al interface strength and softening of Al matrix after annealing at 200 and 300 $^{\circ}\text{C}$ with insignificant intermetallic formation would induce crack propagation through Al away from Cu/Al interface. This would mitigate against crack deviation and deflection to and from Cu/Al interface, resulting in the weaker undulations (or serrations) in the peel stress-displacement curves. Figure 11b, d showed the thick intermetallic compound (marked as “IMC”) formation at the Cu/Al interface. As stated (Fig. 7), the height level of intermetallic/Al interface in the region without Ni interlayer approached the level of Ni/Al interface, that would induce easy crack growth along the intermetallic layers and lower the peel strength.

Figure 12a–d display the EDS elemental map images of fracture surface of peeled off Cu plate with Ni interlayers of 25 μm for the as-roll-bonded (a) and annealed Cu/Al/Cu at 200 $^{\circ}\text{C}$ (b), 300 $^{\circ}\text{C}$ (c) and 400 $^{\circ}\text{C}$ (d). As explained in Fig. 4, the ridge-like pattern in Al developed because crack

Fig. 11 SEM images (a, b) and EDS elemental mapping images (c, d) of separated Cu/Al interface region with 25 μm Ni interlayer annealed at 200 $^{\circ}\text{C}$ (a, c) and 500 $^{\circ}\text{C}$ (b, d) in the partially peeled off clad plate. (Color figure online)

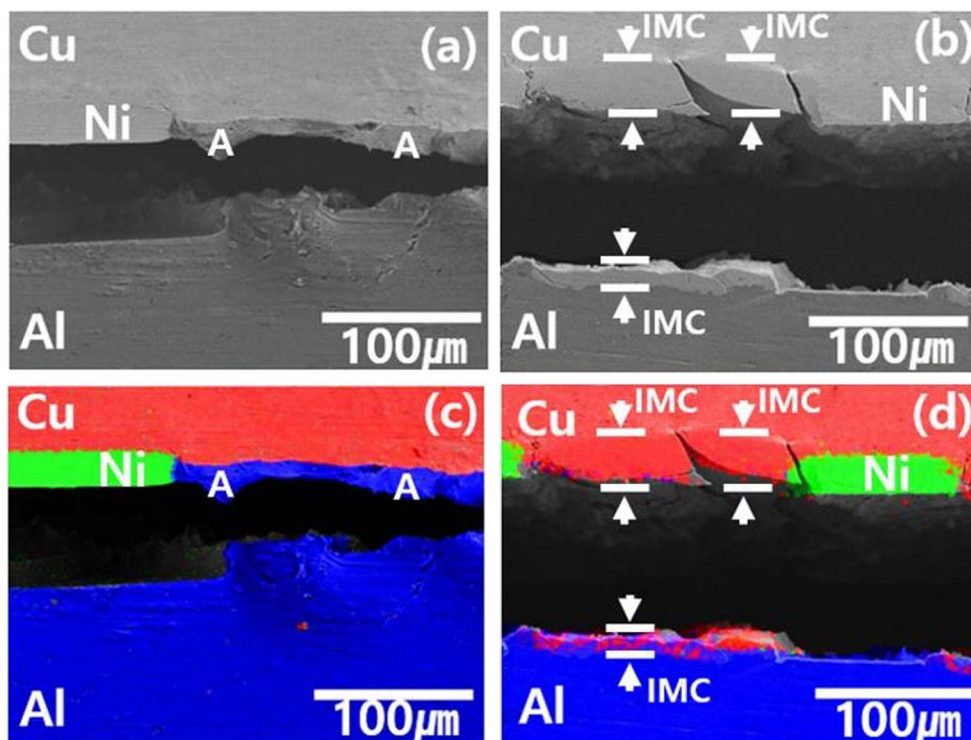
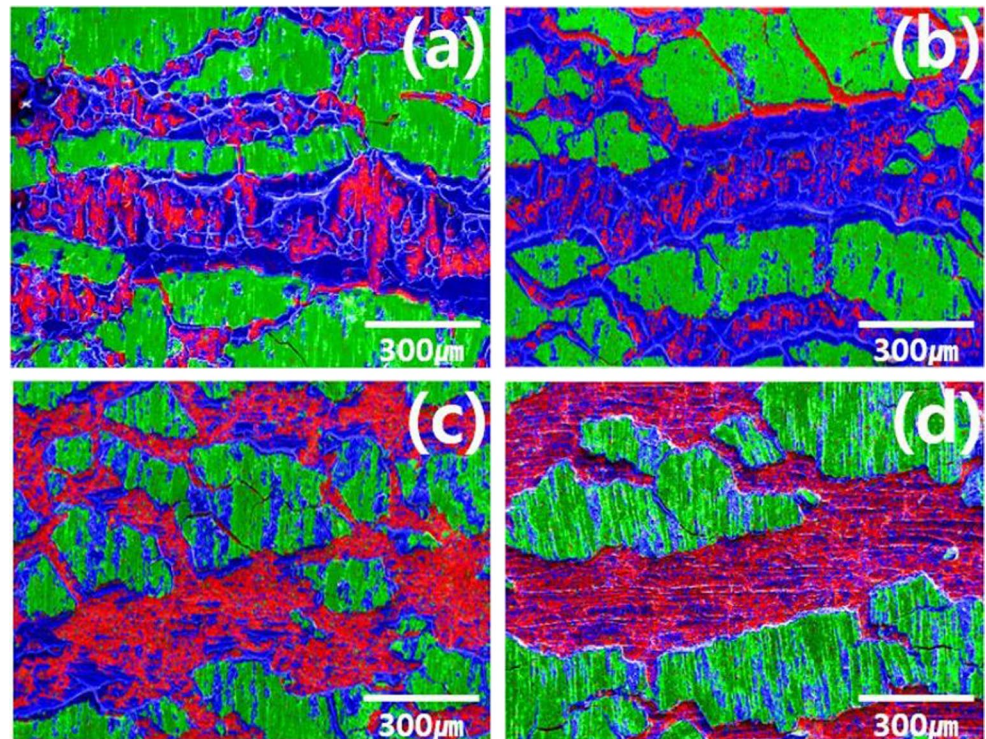


Fig. 12 EDS elemental map images of fracture surface of peeled off Cu plate with Ni interlayers of 25 μm for the as-roll-bonded (a) and annealed Cu/Al/Cu at 200 $^{\circ}\text{C}$ (b), 300 $^{\circ}\text{C}$ (c) and 400 $^{\circ}\text{C}$ (d). (Color figure online)



propagated through Al not along Cu/Al interface because of the strong Cu/Al interfacial bonding. Inter-connected region with the ridge-like pattern in blue (Al) developed more pronouncedly after annealing at 200 $^{\circ}\text{C}$, suggesting the enhanced Cu/Al interfacial bonding after annealing at 200 $^{\circ}\text{C}$. It should be noted that the red areas (Cu) in the region with ridge-like pattern in blue (Al) decreased with annealing at 200 $^{\circ}\text{C}$, supporting the more stable crack propagation through the Al matrix away from the Cu/Al interface and the significant increase of the peel strength. The increase of Al volume attached to the Cu plate after annealing at 200 $^{\circ}\text{C}$ is attributed to the enhanced diffusion bonding between Cu and Al and the enhanced ductility of Al after annealing.

With increase of annealing temperature to 300 $^{\circ}\text{C}$, the blue-colored area in the inter-connected region decreased, implying the appreciable formation of intermetallics consisting of Cu and Al and crack propagation through the intermetallic region. As shown in XRD analyses in Fig. 8, thin Cu_9Al_4 intermetallic layer was formed at the Cu/Al interface at 300 $^{\circ}\text{C}$ [1, 7, 8], attracting the cracks through this thin intermetallic layer. The peel strength after annealing at 300 $^{\circ}\text{C}$ is, however, still greater than that of as-roll-bonded Cu/Al/Cu partly because of the diffusion bonding between Al and Ni and the less brittle nature of thin Cu/Al intermetallics formed at 300 $^{\circ}\text{C}$. As shown in Fig. 12c, more Al (blue) debris is attached to the Ni (green) layer due to the enhanced diffusion bonding between Al and Ni. At 300 $^{\circ}\text{C}$, no brittle intermetallics were observed at the Ni/Al interface

as evidenced from XRD analysis (Fig. 9). After annealing at 400 $^{\circ}\text{C}$, the area fraction of Al (blue) is very small. It was found that Cu_9Al_4 , CuAl CuAl_2 and NiAl_3 intermetallics were formed extensively at the interfaces as supported by XRD (Fig. 9), resulting in the crack propagation through intermetallic layers and the lower peel strength.

In Fig. 13, the average peel strengths of as-roll-bonded and annealed Cu/Al/Cu composite are plotted against the

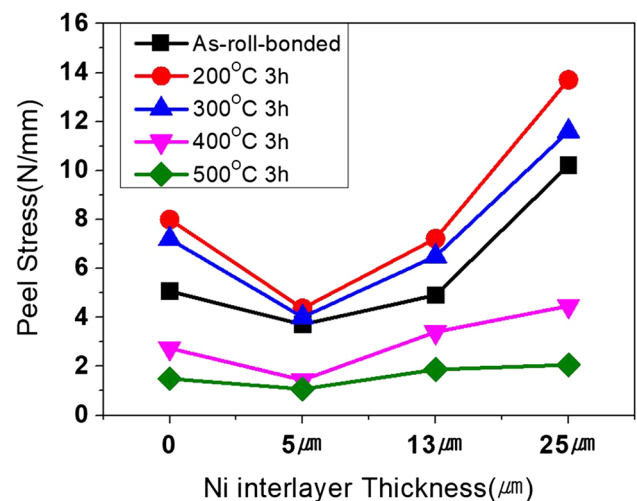


Fig. 13 Average peel strengths of as-roll-bonded and annealed Cu/Al/Cu composite plotted against the Ni interlayer thickness. Peel strengths of Cu/Al/Cu clad without Ni interlayers roll-bonded under the same processing conditions are also plotted

Ni interlayer thickness. The peel strengths of as-roll-bonded and annealed Cu/Al/Cu composite without Ni interlayer are also plotted for comparison. It is shown that the peel strength decreased with the presence of thin Ni interlayer up to 5 μm and then increased rapidly with further increasing Ni interlayer thickness above 10 μm . The peel strength of Cu/Al/Cu annealed at 200 $^{\circ}\text{C}$ increased with increasing Ni interlayer thickness and reached up to 14.5 N/mm for Cu/Al/Cu with 25 μm thick Ni interlayer. On the other hand, the peel strength of Cu/Al/Cu annealed at 400 $^{\circ}\text{C}$ decreased pronouncedly compared to that of as-roll-bonded Cu/Al/Cu composite, suggesting easier interface crack propagation through the brittle intermetallic layers. The highest peel strength (14.5 N/mm) of Cu/Al/Cu clad composite with 25 μm thick Ni interlayer was much higher than those (~ 6 N/mm) observed in Cu/Al clad by Chen et al. [7] and Peng et al. [30]. The peel strength of Cu/Al/Cu composite with 25 μm thick Ni interlayer in the present study is also higher than that (10 N/mm) reported on Cu/Al clad with 30 μm thick Ni interlayer by Shabani et al. [28]. Thermal stability of Cu/Al/Cu composite with 25 μm Ni interlayer after annealing at 400 $^{\circ}\text{C}$ was superior to that of Cu/Al/Cu composite without Ni interlayer. The peel strength of Cu/Al/Cu composite with 25 μm Ni interlayer was found to be 4.6 N/mm after annealing at 400 $^{\circ}\text{C}$, greater than that of Cu/Al/Cu composite without Ni interlayer (2.7 N/mm). The peel strength of Cu/Al/Cu clad composite can be enhanced by the interface design and modification through the variations of size and distribution of Ni interlayers and the enhanced interface bonding.

4 Conclusions

We investigated the effect of interface modification in Cu/Al/Cu clad composite by Ni interlayer and annealing on crack propagation and interface stability and results are summarized as follows:

1. The peel strength of Cu/Al/Cu clad composite was enhanced through the interface modification by Ni interlayer and annealing. The peel strength of as-roll-bonded Cu/Al/Cu with 25 μm thick interlayer reached 11 N/mm and increased to 14.5 N/mm after post-roll-bonding annealing at 200 $^{\circ}\text{C}$.
2. Propagating cracks during the peel test would deflect and deviate away from the Cu/Al interface as the crack approached the region with Ni interlayer because of strong Cu/Ni interface bonding. The deflection of propagating crack away from Cu/Al interface would induce heavy deformation of Al matrix and increase the peel strength.

3. Cu/Al/Cu with 25 μm thick Ni interlayer exhibited the remarkable stress undulation in the peel stress-displacement curves, which can be attributed to the modification of the crack path in the presence of periodic Ni interlayer at the Cu/Al interface. The periodic crack deflection would increase the crack propagation energy, resulting in the enhanced peel strength.
4. Because of the fast growing intermetallic at the Cu/Al interface after heat treatment above 400 $^{\circ}\text{C}$, the height level of intermetallic/Al interface in the region without Ni interlayer approached the level of Ni/Al interface, inducing smooth crack growth along the intermetallic layers and lowering the peel strength.
5. The enhanced Cu/Al interface bonding and softening of Al matrix prevented the crack propagation along the Cu/Al interface and induced cracking through Al matrix after annealing below 300 $^{\circ}\text{C}$, resulting in the substantial increase of peel strength associated with high crack propagation energy.

Acknowledgements This work was supported by the 3rd phase of the Fundamental R&D Programs for Core Technology of Materials funded by Ministry of Trade, Industry and Energy (Grant No. G011005095104).

References

1. M. Kent, *Electr. Veh. Mag.* **27**, 29 (2016)
2. K. Oba, *Fujikura Tech. Rev.* **42**, 77 (2013)
3. A. Uhlemann, A. Herbrandt, *PCIM Europe* **2012**, 680 (2012)
4. S. Park, S. Nagao, T. Sugahara, K. Suganuma, *J. Mater. Sci.* **26**, 7277 (2015)
5. I.K. Kim, S.I. Hong, *Mater. Des.* **47**, 590 (2013)
6. I.K. Kim, S.I. Hong, *Mater. Des.* **57**, 625 (2014)
7. C.Y. Chen, H.L. Chen, W.S. Hwang, *Mater. Trans.* **47**, 1232 (2006)
8. M. Abbasi, A.K. Taheri, M.T. Salehi, *J. Alloys Compd.* **319**, 233 (2001)
9. I.K. Kim, J.S. Ha, S.I. Hong, *Korean J. Met. Mater.* **50**, 939 (2012)
10. J.-S. Kim, J. Park, K.S. Lee, S. Lee, Y.W. Chang, *Met. Mater. Int.* **22**, 771 (2016)
11. J.G. Kim, S.M. Baek, W.T. Cho, T.J. Song, K.G. Chin, S.H. Lee, H.S. Kim, *Met. Mater. Int.* **23**, 459 (2017)
12. Y.B. Zhang, Y. Fu, J.C. Jie, L. Wu, K. S. Q.T. Guo, T.J. Li, T.M. Wang, *Met. Mater. Int.* **23**, 1197 (2017)
13. M.M. Hoseini-Athar, B. Tolaminejad, *Met. Mater. Int.* **22**, 670 (2016)
14. D.H. Lee, J.S. Kim, H.J. Song, S.H. Lee, *Met. Mater. Int.* **23**, 805 (2017)
15. J.H. Cha, S.H. Kim, Y.S. Lee, H.W. Kim, Y.S. Choi, *Met. Mater. Int.* **22**, 880 (2016)
16. H.L. Yu, C. Lu, A.K. Tieu, H.J. Li, A.R. Godbole, C. Kong, *Philos. Mag.* **98**, 1537 (2018)
17. H.T. Gao, X.H. Liu, J.L. Qi, Z.R. Ai, L.Z. Liu, *J. Mater. Process. Technol.* **251**, 1 (2018)
18. B. Guan, B.Y. Chen, Y. Zang, Q. Qin, *Strength Mater.* **50**, 79 (2018)

19. F. Moisy, A. Gueydan, X. Sauvage, A. Guillet, C. Keller, E. Guilmeau, E. Hug, *Mater Des.* **155**, 366 (2018)
20. Q. Zhang, S. Li, J. Liu, Y. Wang, B. Zhang, L.Y. Zhang, *Metals* **8**, 329 (2018)
21. C. Yu, Z.C. Qi, H. Yu, C. Xu, H. Xiao, *J. Mater. Eng. Perform.* **27**, 1664 (2018)
22. K.S. Lee, S.M. Lee, J.S. Lee, Y.B. Kim, G.A. Lee, S.P. Lee, D.S. Bae, *Met. Mater. Int.* **22**, 880 (2016)
23. E. Hug, N. Bellido, *Mater. Sci. Eng. A* **528**, 7103 (2011)
24. I.K. Kim, S.I. Hong, *Metall. Mater. Trans. A* **44**, 3890 (2014)
25. J.G. Kim, J.H. Ju, D.Y. Kim, S.H. Park, Y.R. Cho, *Korean J Met. Mater.* **55**, 523 (2017)
26. J.Y. Jin, S.I. Hong, *Mater. Sci. Eng. A* **596**, 1 (2014)
27. H. Paul, L.L. Dobrzyńska, *Metall. Mater. Trans. A* **44**, 3836 (2013)
28. A. Shabani, M.R. Toroghinejad, A. Shafyei, *Mater. Des.* **40**, 212 (2012)
29. J. Zhang, G. Luo, Y. Wang, Q. Shen, L. Zhang, *Mater. Lett.* **83**, 189 (2012)
30. X.K. Peng, R. Wuhler, G. Heness, W.Y. Yeung, *J. Mater. Sci.* **35**, 4357 (2000)
31. J.R. Tuck, A.M. Korsunsky, R.I. Davidson, S.J. Bull, D.M. Elliott, *Surf. Coat. Technol.* **127**, 1 (2000)
32. C. Barret, T.B. Massalski, *Structure of Metals*, third ed., revised edn. (Pergamon Press, Oxford, 1980), p. 545
33. S.I. Hong, M.A. Hill, *Acta Mater.* **46**, 4111 (1998)
34. S.I. Hong, M.A. Hill, *Mater. Sci. Eng. A* **281**, 189 (2000)
35. K.H. Lee, S.I. Hong, *J. Mater. Res.* **18**, 2194 (2003)
36. S.I. Hong, *Mater. Sci. Eng. A* **711**, 492 (2018)
37. W.N. Kim, S.I. Hong, *Mater. Sci. Eng. A* **651**, 976 (2016)